$$(-i)^l \lim_{\epsilon\to 0} \frac{(-1)^m\Gamma(b)\Gamma(\lambda+3-m)}{2(2\pi)^{\frac{1}{2}}i^{(l+m)}\Gamma(a)\Gamma(b-a)} \int_{-\infty}^{\infty} dp \int_{-1}^{1} ds \int_{0}^{1} dt \times P_l(s)s^{-m}(\epsilon+c-ct-ips)^{m-\lambda-3}\tilde{G}_{lm}{}^{(m)}(k,p) \times t^{a-1}(1-t)^{b-a-1}, \quad \text{(B-34)}$$

by the same manipulations as were used to obtain Eq. (B-26). But except for the factor $(-i)^l$, this is identical with the integral of (B-26), with $n=0$, $c=d$, and $G_l(p)$ replaced by $G_{lm}(k,p)$. Consequently the remainder of the proof follows identically the proof of Theorem (B-1).

PHYSICAL REVIEW VOLUME 116, NUMBER 5 DECEMBER 1, 1959

Scattering of 18-Mev Alpha Particles by C^{12}, O^{16}, and S^{32}†

J. C. CORELLI,* E. BLEULER, AND D. J. TENDAM
Department of Physics, Purdue University, Lafayette, Indiana

(Received July 15, 1959)

The scattering of 18-Mev alpha particles by gaseous C_3H_8, O_2, and H_2S targets was studied with a multiplate scattering chamber. The elastic angular distributions exhibit the diffraction-like pattern typical of light elements. Carbon and oxygen show a sharp rise above the Rutherford cross sections at the backward angles, with values σ/σ_R of 660 for carbon and 350 for oxygen near 173°. A good fit to the angular distribution for inelastic scattering leading to the first excited state of C^{12} (4.43 Mev, 2^+) is obtained using a $[j_2(qR)]^2$ dependence with $R=5.5\times10^{-13}$ cm. No direct-interaction analysis is possible for the alpha-particle groups corresponding to the 7.65-Mev and 9.61-Mev levels in C^{12} and to the excited states of O^{16} up to the 8.87-Mev level. All these distributions show strong forward peaking. In the case of inelastic scattering by S^{32} ($Q=-2.44$ Mev), an interaction radius of 6.5×10^{-13} cm can be deduced from the angular distribution, though the agreement with $[j_2(qR)]^2$ is rather poor. A summary of elastic scattering results for elements in the range from $Z=6$ to $Z=47$ is presented. Expressions for the second-order geometry and the multiple-scattering corrections are given.

I. INTRODUCTION

THIS investigation is part of a program to study the scattering of 18- to 19-Mev alpha particles by light and medium-heavy nuclei. The scattering cross sections of Ne, Al, A, Cu, and Ag have been discussed in earlier reports.[1–3] In the present study, C, O, and S were investigated. The carbon and oxygen targets were chosen because the elastic cross section for neon had shown a significant rise at large angles and it seemed desirable to check this trend at lower Z. Sulfur was included as one of the heavier $n\alpha$-type nuclei and because it was hoped that eventually an accurate theory might allow the determination of the nuclear deformation from the angular distribution of the inelastically scattered alpha particles leaving S^{32} in its first excited state.[4]

With the present measurements, a fairly complete survey of the elastic alpha-particle scattering at 18 to 19 Mev is now available in the range of elements from $Z=6$ to $Z=47$.

II. EXPERIMENTAL PROCEDURE

The experimental methods used were essentially those described by Seidlitz *et al.*[2] The external alpha-particle beam of the 37-inch cyclotron was focused by means of a magnetic quadrupole lens into a 19-inch diameter scattering chamber and collimated within a cone of 0.56° half-angle before passing through the target. The beam was collected by a Faraday cup and measured with an integrator of the type designed by Higinbotham and Rankowitz.[5] The maximum error in the number of incident alpha particles is 1.5%. The average incident alpha-partcle energy was obtained, with an estimated maximum error of 1%, by measuring the mean range in aluminum.[6]

The target materials used were reagent grade propane (C_3H_8), oxygen (O_2) and hydrogen sulfide (H_2S), and, for one auxiliary run, a polyethylene foil. The gases were contained in a brass target cell with a $\frac{1}{2}$-mil thick Mylar window, described in detail by Corelli *et al.*[7] The metal parts of the target cell did not obstruct the paths of particles scattered in the range of angles from 10°

† Work supported in part by the U. S. Atomic Energy Commission. This article is based on a doctoral thesis submitted by J. C. Corelli to the faculty of Purdue University. Preliminary reports have been given in Bull. Am. Phys. Soc. Ser. II, 2, 34 (1957), and Ser. II, 3, 199, 200 (1958).

* Now at Knolls Atomic Power Laboratory, Schenectady, New York.

[1] E. Bleuler and D. J. Tendam, Phys. Rev. **99**, 1605 (1955).

[2] Seidlitz, Bleuler, and Tendam, Phys. Rev. **110**, 682 (1958); (references to earlier work are cited therein).

[3] Gailar, Bleuler, and Tendam, Phys. Rev. **112**, 1989 (1958).

[4] S. Hayakawa and S. Yoshida, Proc. Phys. Soc. (London) **A68**, 656 (1955). S. Hayakawa and S. Yoshida, Progr. Theoret. Phys. (Kyoto) **14**, 1 (1955).

[5] W. A. Higinbotham and S. Rankowitz, Rev. Sci. Instr. **22**, 688 (1951).

[6] Gailar, Seidlitz, Bleuler, and Tendam, Rev. Sci. Instr. **24**, 126 (1953).

[7] Corelli, Livingston, and Seidlitz, Rev. Sci. Instr. **28**, 471 (1957).

to 170°. For all gas targets the absolute pressure used was nominally 10 cm Hg; it was measured to within ± 0.05 mm by means of a mercury manometer using a cathetometer. The temperature of the gas was measured to ± 0.1°C with a thermometer which was kept in thermal contact with the base of the target cell.

Scattered alpha particles were selected at 63 angles by means of an analyzing slit system (see Fig. 1). The nominal scattering angles were spaced 2.5°, the slits allowed maximum deviations of 0.96° from the nominal angles (in the nominal scattering plane). The slit system was checked for inhomogeneities by measuring the relative transmission of alpha particles from a Po source through each slit, at six different positions along the slit. The corrections for slit-width variations which have been applied to all data to be presented amounted to only 1% to 5%.

The scattered particles were detected in 63 nuclear track plates, 1×3 inch, with 100-μ Ilford E-1 emulsion. Particle discrimination between scattered alphas and reaction protons and deuterons was accomplished by a differential development[8] and fading technique.[2]

In order to measure track lengths rapidly, specially constructed eyepiece reticles were used. These consisted of rectangular arrays of 100 vertical divisions with the fifth and tenth lines accented, which in the field of view appeared as a miniature "football field" with each yard marked off by a stripe. A stage micrometer calibrated with an Abbe comparator was used to obtain the number of microns per division. The scale height which defined a scan width was equivalent to 70 divisions and was known to better than 0.5%.

A monitor counter was installed at 34° in order to measure the spectra of particles scattered by the target during the exposure of the plates. Particles scattered into the monitor were detected by a scintillation counter consisting of a thin CsI(Tl) crystal directly coupled to a Dumont-6292 photomultiplier. The resulting pulses were delivered to a 20-channel analyzer. The main purpose of the monitor was to check the target content for the possible appearance of contamination peaks. In addition to this it served as a check on the proper operation of the current integrator.

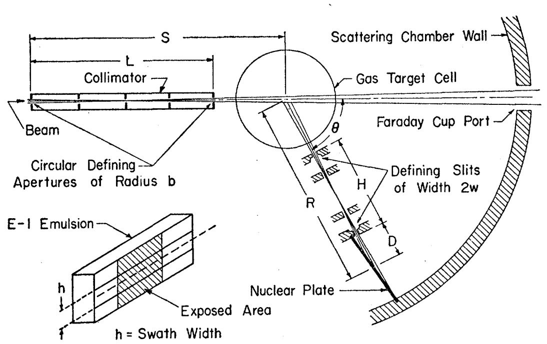

FIG. 1. Scattering geometry in the nominal scattering plane.

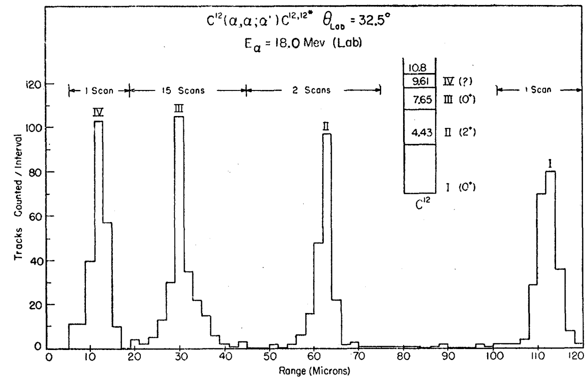

FIG. 2. Range distribution of alpha particles scattered by carbon.

III. ANALYSIS OF DATA

1. Alpha-Particle Spectra

For each plate a track-length distribution was plotted and the groups were correlated with the various levels of the scattering nucleus. The ranges of scattered alpha particles in the emulsion always agreed very well with the values calculated using the range-energy curve given by Rotblat.[9] In Fig. 2 is shown a typical histogram of the range distribution of alpha particles scattered by carbon into the 32.5° plate. The groups easily resolved correspond to the scattering of alpha particles from the ground state (0^+), the first excited state at 4.43 Mev (2^+), the second excited state at 7.65 Mev (0^+), and the third excited state at 9.61 Mev (?) excitation energy. The excitation energies, spins, and parities were taken from the review article of Ajzenberg and Lauritsen.[10]

Figure 3 shows the range distribution of alpha particles scattered by the gaseous oxygen target into the 60° plate. In addition to the elastic group (I), we obtain groups from the unresolved doublets of the 1st and 2nd excited states at 6.06 and 6.13 Mev, (II) and of the 3rd and 4th excited states at 6.91 and 7.12 Mev (III). Also present, though less well isolated, is the level at 8.87 Mev (IV),[11,12] which is definitely in evidence on all plates up to 75°.

Figure 4 shows the spectrum of alpha particles scattered into the 167.5° plate together with the spectrum of particles scattered into the monitor (at 34°) when hydrogen sulfide was bombarded with alpha particles. A small amount of air contaminant is present as is evident from the elastic peaks from N^{14} and O^{16} in both the nuclear plate and monitor. However, since

[8] Roberts, Solano, Wood, and Billington, Rev. Sci. Instr. **24**, 920 (1953).

[9] J. Rotblat, Nature **167**, 550 (1951).

[10] F. Ajzenberg and T. Lauritsen, Revs. Modern Phys. **27**, 77 (1955).

[11] W. F. Hornyak and R. Sherr, Phys. Rev. **100**, 1409 (1955).

[12] Wilkinson, Toppel, and Alburger, Phys. Rev. **101**, 673 (1956).

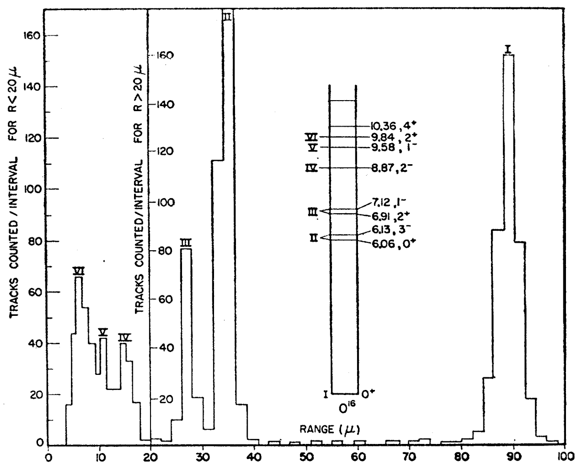

FIG. 3. Range distribution of alpha particles scattered by oxygen; $E_\alpha = 18.3$ Mev, $\theta_{\text{lab}} = 60°$. *Note.* "Range ($\mu$)" at the bottom of the figure should read "Range (μ, microns)."

the cross section for the elastic scattering of alpha particles by oxygen had been measured, the amount of contaminant could be computed (16.5%) and subtracted in obtaining the final absolute cross sections. The presence of the contamination peak did not warrant analysis for excited states of S^{32} higher than the first at 2.24 Mev (2^+). The elastic peak from sulfur in the monitor [Fig. 4(a)] was observed to be constant (per unit of charge collected in the Faraday cup) during the whole run, indicating that the decomposition of the H_2S by the beam was negligible.

2. Calculation of Cross Sections

If $Y(\theta)$ is the number of scattered particles in a particular group, obtained by scanning the length of the plate over a swath width h, an uncorrected differential cross section $\bar{\sigma}(\theta)$ is calculated from the formula

$$Y(\theta) = \frac{Nn4w^2h}{HR\sin\theta}\bar{\sigma}(\theta). \tag{1}$$

The true cross section $\sigma(\theta)$ is given by

$$\bar{\sigma}(\theta) = \sigma(\theta)(1+\Delta_g+\Delta_m). \tag{2}$$

The geometric quantities H, R, w, and θ are shown in Fig. 1, N is the number of scattering nuclei per unit volume, n the number of alpha particles that traversed the target. The correction terms Δ_g and Δ_m which account for the effects of finite geometry and multiple scattering are derived in the Appendix. These corrections were applied to all elastic scattering data. The relative derivatives of the true cross section, σ'/σ and σ''/σ, needed for the calculation of Δ_g and Δ_m, were approximated by the relative derivatives of the uncorrected cross section, $\bar{\sigma}'/\bar{\sigma}$ and $\bar{\sigma}''/\bar{\sigma}$, except near the deep minima. In order to obtain $\bar{\sigma}'$ and $\bar{\sigma}''$ each peak in the angular distribution was expressed by a power series in $\sin(\theta-\theta_{\max})$ with coefficients determined by a least-squares fit. The total corrections $(\Delta_g+\Delta_m)$ thus calculated were always less than 4%. Near the deep minima, a parabolic dependence of the true cross section on angle was assumed and its parameters were determined from the experimental values of $\bar{\sigma}$. Differences up to 30% between σ and $\bar{\sigma}$ were found in the backward minima for C and O, where the energy of the scattered alpha particles is small, causing a large mean square multiple-scattering angle.

The nominal scattering angles, θ, i.e., the angles between the collimator axis and a line passing through the centers of the detector slits, were known within

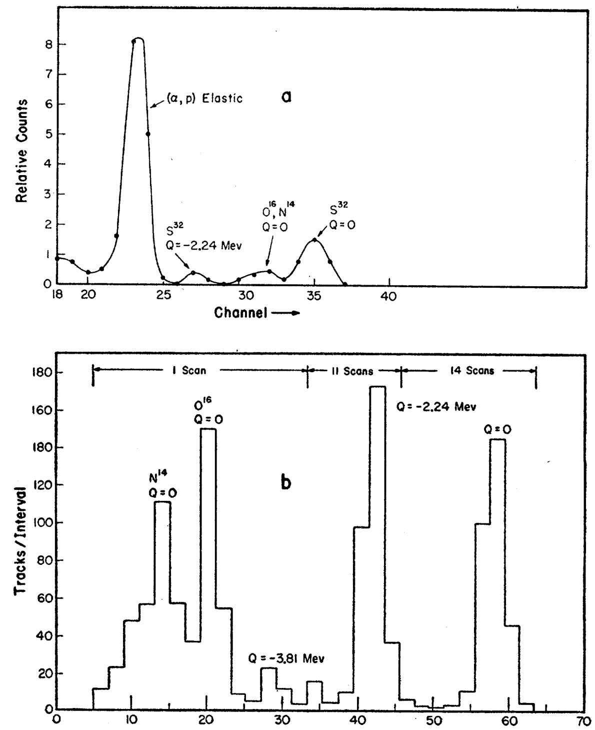

FIG. 4. Scattering by H_2S. (a) Pulse-height distribution in CsI monitor at $\theta = 34°$. Note the peak due to elastic scattering from N, O contamination. (b) Range distribution in the 167.5° plate. Since the cross sections of N and O are very high at large angles, an accurate determination of the contamination is possible.

0.05°. A possible zero shift due to nonaxial passage of the beam through the collimator was checked with the aid of two symmetrically located plates (at 20° left and right). The cross sections measured by these two plates differed by an amount which could be attributed to zero shifts of 0.1° for all experiments. No correction was applied to the scattering angle or to the intensity since it would have been small and uncertain, because the asymmetry could arise from shifts of both the position and the direction of the most intense part of the beam.

Possible systematic errors of the number of tracks counted, $Y(\theta)$, are due to the analysis of neighboring groups and to the treatment of the background between the prominent groups (see Figs. 2 and 3). Though most of it probably arises from inelastic scattering by the rarer isotopes, part of it may be due to alpha particles that are degraded in energy by scattering in the beam pipe and the collimator and then elastically scattered in the target. The degraded beam would be measured in the current integrator, contributing to n in Eq. (1), whereas the scattered particles would not be counted in the main groups and would not contribute to $Y(\theta)$. The value of $\bar{\sigma}(\theta)$ obtained, then, would be too low. The error may be as high as 3% for the elastic groups. The statistical errors of the number of tracks counted, $Y(\theta)$, is 5–6% for the elastic groups with few exceptions where the intensity is very low. The statistical errors for the inelastic groups are indicated in the graphs of the cross sections.

All data to be presented in the following section have been transformed to the center-of-mass system.

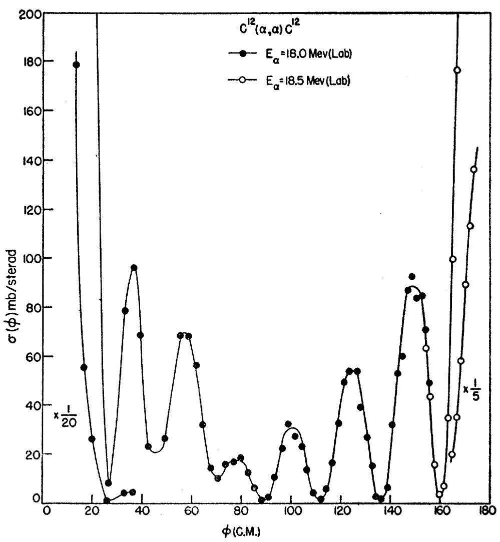

FIG. 5. Elastic scattering of 18.0-Mev and 18.5-Mev alpha particles by carbon.

IV. EXPERIMENTAL RESULTS

1. Elastic Scattering

The angular distribution for the elastic scattering of 18.0- and 18.5-Mev alpha particles by carbon is shown in Fig. 5. For scattering angles less than or equal to 156° the target used was propane (C_3H_8). For these data the incident energy (at the center of the gas target) was 18.0 Mev. At larger angles the scattered alpha particles, having lost a large fraction of their energy in the collision, did not emerge from the gas cell. Hence in order to examine the scattering from these angles a 0.38±0.020 mil polyethylene foil[13] was used as the target in a second run. In this case only a

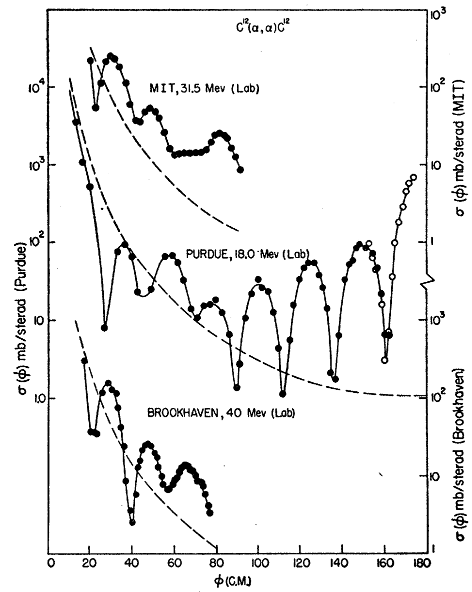

FIG. 6. Elastic scattering of 18.0-Mev, 31.5-Mev, and 40-Mev alpha particles by carbon. – – – – – – Rutherford cross sections. Note the different scales.

single outer ring of a new analyzing slit system was used to define the scattering particles. The mean energy in the target was 18.5 Mev. In the region where the two runs overlap, the cross sections found agree very well.

Figure 6 shows the angular distribution for elastic scattering of alpha particles by carbon at various incident energies. Included are measurements made by

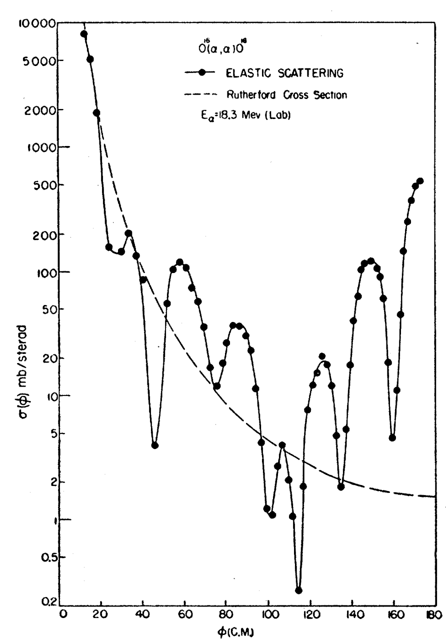

FIG. 7. Elastic scattering of 18.3-Mev alpha particles by oxygen.

[13] Kindly supplied and prepared for us by Bakelite Company, Division of Union Carbide Corporation, Bound Brook, New Jersey.

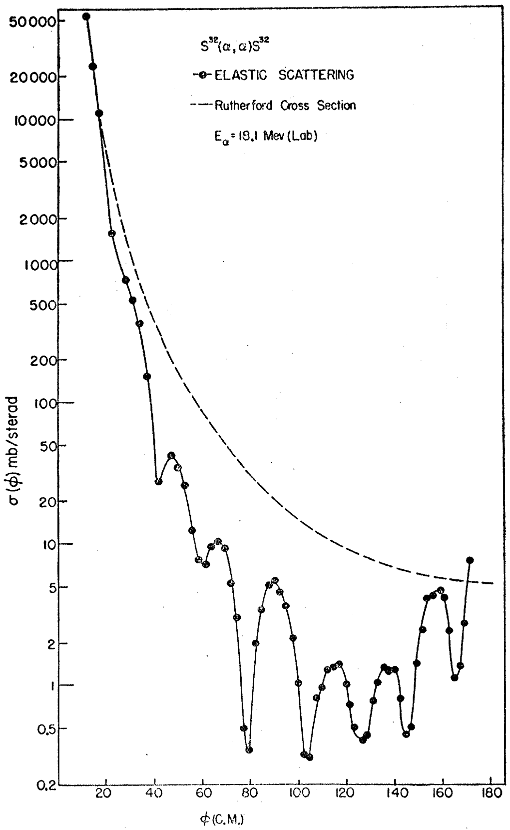

FIG. 8. Elastic scattering of 18.1-Mev alpha particles by sulfur.

Watters[14] (MIT), and by Igo, Wegner, and Eisberg[15] (Brookhaven), using incident alpha-particle energies of 31.5 Mev and 40 Mev, respectively. The comparison of the three angular distributions shows in general the expected similarity of the patterns with a shift of the diffraction minima to smaller angles as the energy is increased. The rather anomalous behavior in the cross section observed by Watters from 60° to 80° does not appear at our energy nor does it appear at 40 Mev. This peculiarity may be characteristic of the incident energy, in which case the theoretical interpretation would appear to be difficult. In our distribution the strong upward shift in the pattern for $\phi > 100°$ is very remarkable. At $\phi = 173°$ the ratio of the experimental cross section to the (18-Mev) Rutherford cross section is $\sigma/\sigma_R = 660$.

The differential cross section as a function of scattering angle for elastic scattering of 18.3-Mev alpha particles from oxygen together with the Rutherford cross section is given in Fig. 7. The similarity between this angular distribution and that of carbon is evident. At an angle of 172.5° the ratio $\sigma/\sigma_R = 350$.

The angular distribution for elastic scattering of 18.1-Mev alphas by sulfur is shown in Fig. 8. The appearance of the diffraction pattern resembles closely that measured by Seidlitz[2] for the scattering of 18-Mev alpha particles by argon. Beyond about 20° the cross section is always smaller than the Rutherford cross section except at 172°.

2. Inelastic Scattering

For carbon, angular distributions for the inelastically scattered groups II, III, and IV (Fig. 2) were obtained. Figure 9 shows a comparison for group II, which leaves C^{12} in its first excited state (2^+) at 4.43 Mev, with measurements by Watters[14] at 31.5 Mev. The two distributions are similar, with the expected contraction of the pattern at the higher energy. The cross sections at

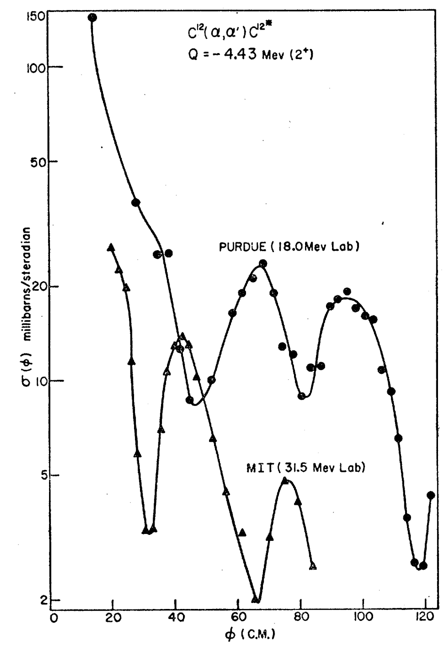

FIG. 9. Inelastic scattering of 18.0-Mev and 31.5-Mev alpha particles by carbon ($Q = -4.43$ Mev).

the maxima are 2 to 4 times higher for 18.1-Mev than for 31.5-Mev alpha particles. Applying the simplified formulas of the various direct-interaction theories,[4,16,17] an attempt is made in Fig. 10 to fit the angular distribution with the function $[j_2(qR)]^2$ where q is the magnitude of the change in wave vector of the system and R an interaction radius. A fair fit is obtained for $R = 5.5 \times 10^{-13}$ cm.

For group III ($Q = -7.65$, 0^+ state of C^{12}), the angular distribution at 18.0 Mev is rather different from that at 31.5 Mev, though it shows the same forward peaking (Fig. 11). Watters' curve agrees fairly well with a $[j_0(qR)]^2$ distribution, but no such fit is possible in our

[14] H. J. Watters, Phys. Rev. **103**, 1763 (1956).
[15] Igo, Wegner, and Eisberg, Phys. Rev. **101**, 1508 (1956).
[16] Austern, Butler, and McManus, Phys. Rev. **92**, 350 (1953).
[17] S. T. Butler, Phys. Rev. **106**, 272 (1957).

case. Again, the cross section is somewhat higher at the lower energy; it is a factor ten lower than that for group II. A similarly low cross section for a 0^+-0^+ excitation had been observed by Seidlitz *et al.* in neon.[2]

The spin and the parity of the third excited state at 9.61 Mev are not known and the angular distribution of the corresponding alpha-particle group, shown in Fig. 12, does not give any clue, exhibiting only a strong monotonic decrease in intensity.

The angular distributions of the three distinct alpha-particle groups arising from inelastic scatterings by oxygen (groups II, III, IV of Fig. 3) are shown in Fig. 13. The similarity of the patterns for groups II and III, each corresponding to doublets of excited states at 6 and 7 Mev, is rather striking in view of the

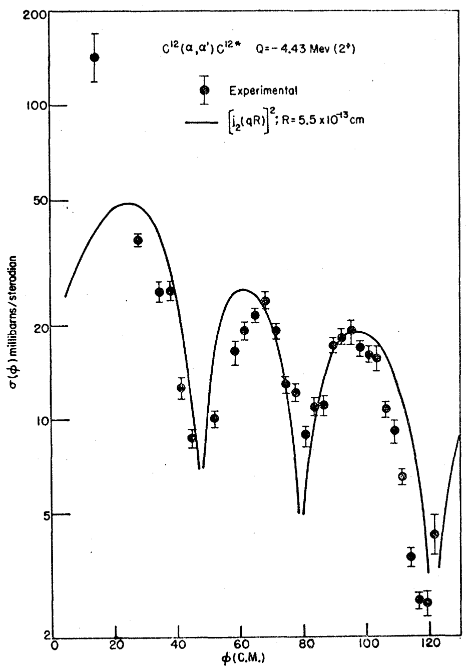

FIG. 10. Inelastic scattering of 18.0-Mev alpha particles by C^{12}; comparison with direct-interaction theory.

different spins and parities of the states involved. No comparison with the direct-interaction formulas has been attempted since each curve would have to be a superposition of the squares of two spherical Bessel functions (j_0 and j_3 for group II; j_1 and j_2 for group III) with not necessarily identical interaction radii. The excitation of the 2^- level at 8.87 Mev cannot occur by a direct interaction of the type normally considered, but the sharp forward peaking appears to indicate a mechanism other than a compound-nucleus process.

Figure 14 shows the angular distribution of the alpha-particle group leaving the S^{32} nucleus in its first excited state (2^+, 2.24 Mev). The arrows indicate the zeros of $j_2(qR)$, with $R=6.5\times10^{-13}$ cm. They are seen to correspond fairly well to the minima of the cross section,

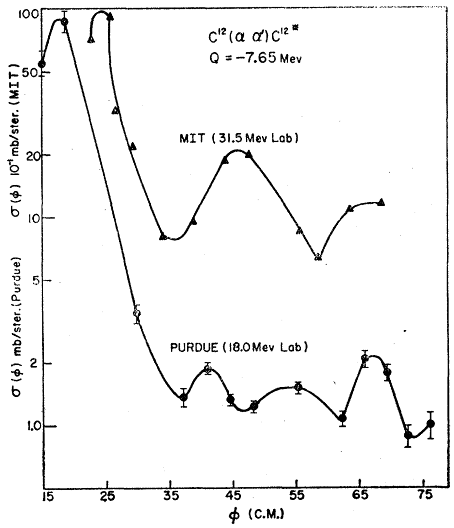

FIG. 11. Inelastic scattering of 18.0-Mev and 31.5-Mev alpha particles by carbon ($Q=-7.65$ Mev). Note scale difference.

but the shape of the experimental curve is in poor agreement with a $[j_2(qR)]^2$ dependence (Fig. 15).

V. DISCUSSION AND SUMMARY

The angular distributions of elastically scattered alpha particles of 18 to 18.7 Mev measured thus far in our laboratory are combined in Fig. 16. The curves for Al, Cu, and Ag were obtained by Gailar *et al.*[3] by counting methods, using E, dE/dx coincidences to distinguish scattered alpha particles from reaction deuterons and protons. For all other nuclei, photographic registration was employed. The results summarized in Fig. 16 are

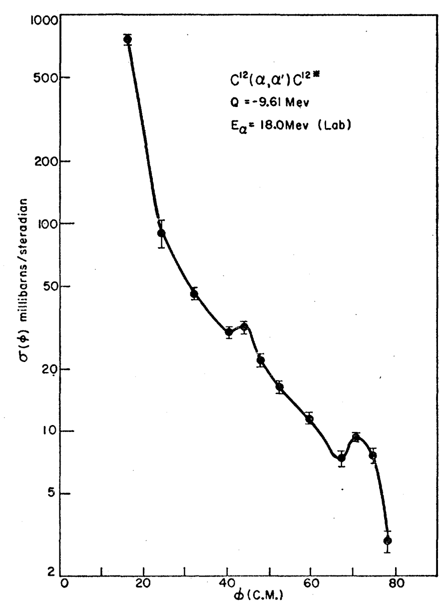

FIG. 12. Inelastic scattering of 18.0-Mev alpha particles by carbon ($Q=-9.61$ Mev).

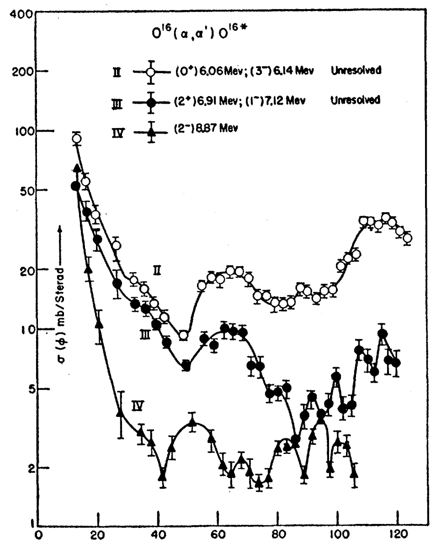

FIG. 13. Inelastic scattering of 18.3-Mev alpha particles by oxygen.

very similar to those obtained by Igo *et al.*[15] with 40-Mev alpha particles, insofar as they show the transition from the "exponential" decrease of σ/σ_R at higher Z to the diffraction-type pattern at lower Z. However, Igo *et al.* do not obtain the huge peaks in the cross sections at the backward angles for carbon since their measurements do not cover as wide a range in angle as ours. In the backward direction the cross sections tend to rise higher, the lower the atomic number. This rise is superimposed on a pronounced oscillatory pattern for all even-even nuclei investigated, whereas irregular fluctuations only show up for aluminum. A similar, but somewhat flatter rise, without the pronounced minima, has been observed for the scattering of 10- to 20-Mev protons by carbon[18] and aluminum.[19] The difference in the patterns seems to be in agreement with optical-model calculations,[20] where deep minima are obtained if central potentials only are used—appropriate to the scattering of alpha particles by even-even nuclei—whereas the inclusion of a spin-orbit term leads to the smoother patterns observed in proton scattering.[21]

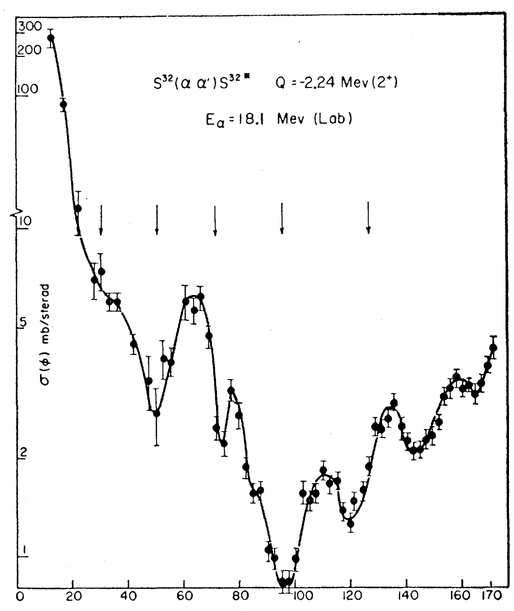

FIG. 14. Inelastic scattering of 18.1-Mev alpha particles by sulfur ($Q=-2.24$ Mev). The arrows indicate the zeros of $j_2(qR)$ for $R=6.5\times10^{-13}$ cm.

Without an optical-model analysis the only quantities that can be determined from the elastic scattering curves are the "diffraction radii," calculated from the formula for the diffraction scattering by an opaque

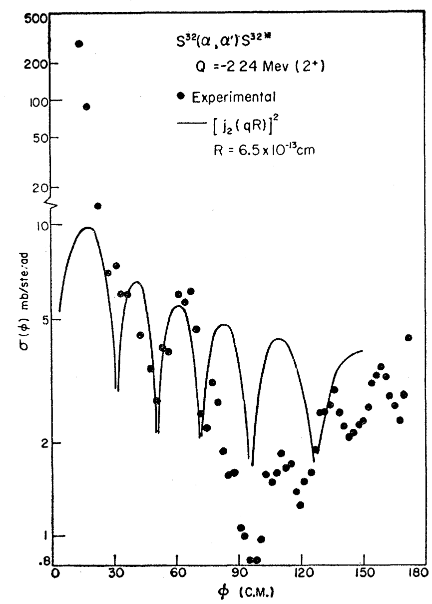

FIG. 15. Inelastic scattering of 18.1-Mev alpha particles by S^{32} comparison with direct-interaction theory.

disk. In this case, $R=\pi/[2k\Delta(\sin(\phi/2))]$ where $\Delta(\sin(\phi/2))$ is the average distance between neighboring minima or maxima in the diffraction pattern, with $\sin(\phi/2)$ as the abscissa. Using the forward quadrant only, one finds values of 7.9×10^{-13} cm (C), 4.35×10^{-13} cm (O), and 6.7×10^{-13} cm (S). The diffraction radii are larger than the mean optical-model interaction radii, but are presumably correlated to them. The values of diffraction radii quoted by Seidlitz *et al.*[2] for Ne, Al, and A are close to $R=(1.5A^{1/3}+2.0)\times10^{-13}$ cm. With this relation the values of R expected for C, O, and S would be 5.44×10^{-13}, 5.78×10^{-13}, and 6.76×10^{-13} cm,

[18] R. W. Peele, Phys. Rev. **105**, 1311 (1957).
[19] I. E. Dayton and G. Schrank, Phys. Rev. **101**, 1358 (1956).
[20] A. E. Glassgold and P. J. Kellogg, Phys. Rev. **107**, 1372 (1957).
[21] F. Bjorklund and S. Fernbach (unpublished), quoted by A. E. Glassgold, Revs. Modern Phys. **30**, 419 (1958).

respectively. The experimental value for S fits the general trend well, but the oxygen radius seems to be exceptionally small, the radius of carbon exceptionally large. It is clear, however, that these qualitative observations should not be given too much weight, especially in view of the evidence from inelastic scattering.

The only inelastic-scattering angular distributions that can be interpreted easily are those corresponding to

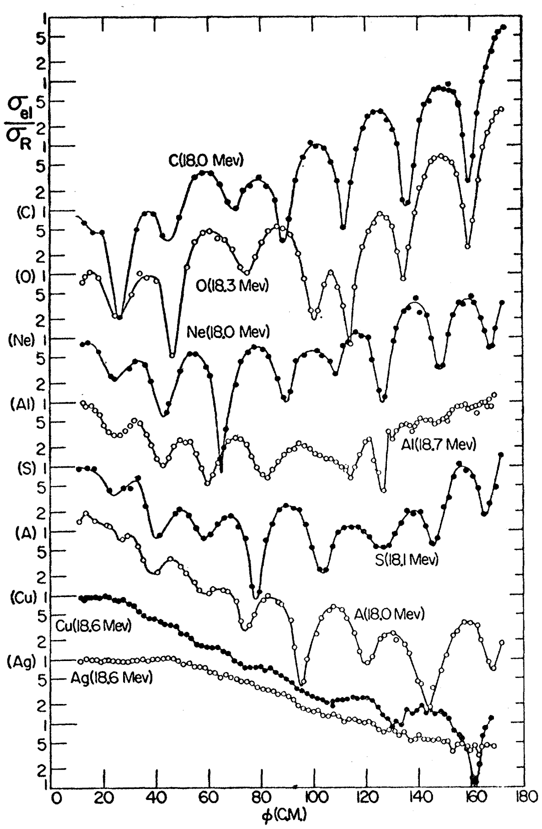

FIG. 16. Survey of elastic scattering of 18- to 18.7-Mev alpha particles, C, O, and S: this work; Ne and A: Seidlitz *et al.*[2]; Al, Cu, and Ag: Gailar *et al.*[3] The mean range of 19.0-Mev alpha particles in Al was recently redetermined with the aid of a new beam-analyzing magnet (47.3 ± 0.1 mg/cm^2). This lead to a 0.1-Mev reduction of the energy values quoted by Gailar *et al.* The energies given by Seidlitz *et al.* are unchanged since the error is accidentally compensated by newer values of the stopping power of the target gases. A recalculation of the second-order geometry and multiple-scattering corrections for Ne and A reduced the cross sections near the minima appreciably below the original values.[2]

the excitation of the first excited, 2^+, states in C^{12} and S^{32}. For sulfur, the interaction radius obtained, 6.5×10^{-13} cm, is close to the above estimate from the elastic scattering. For carbon, however, the much smaller (and more reasonable) value of 5.5×10^{-13} cm is derived which agrees with the value used by Watters[14] at 31.5 Mev. In both cases the angular distribution differs from a simple $[j_2(qR)]^2$ dependence by showing a very high intensity in the forward direction. The same behavior was found by Seidlitz *et al.*[2] for neon and argon. For sulfur, in addition to a generally poor agreement of the details of the patterns, a rise at large angles is observed. It is not known whether these deviations could be removed by a calculation which would use distorted instead of plane waves or whether more than one reaction mechanism would have to be invoked.

ACKNOWLEDGMENTS

The authors take pleasure in expressing their appreciation to Mr. F. Hobaugh and Mr. E. L. Robinson for the cyclotron bombardments, to Mr. J. Moore for his helpful advice in all mechanical problems, and to Mr. J. R. Priest for his aid in the performance and analysis of the carbon experiment. One of us (J.C.C.) would like to acknowledge the use of a least-squares-fit code for an IBM-704 made available by Mr. E. D. Reilly of the Knolls Atomic Power Laboratory. Our special thanks go to Mr. M. Livingston, Mrs. A. Sakahara, Mrs. J. Moore, and Mrs. G. Marks for their meticulous and conscientious scanning of the nuclear plates.

APPENDIX A. GEOMETRY CORRECTION

An expression for the intensity measured in our geometry along a swath of height h has been given by Allred *et al.*[22] It is incomplete, however, insofar as only corrections due to the finite widths of the slits are considered, whereas the spread of the incident beam, the height of the swath scanned, and the angular variation of the cross section are neglected. These effects have been taken into account by Critchfield and Dodder.[23] They assume that the incident beam fills the first circular aperture of the collimator with a uniform spatial and directional distribution. The distribution of the cyclotron beam is not quite so uniformly random, but the description is certainly much better than one based on the assumption of a parallel beam. The formula of Critchfield and Dodder is not immediately applicable, however, because it was calculated for a circular detector aperture located at the position of our second slit. The corrections were recalculated for our geometry following closely the treatment given by Critchfield and Dodder. The final expression for the number of recorded particles is

$$Y(\theta)=\frac{Nn4w^2h}{HR\sin\theta}(1+\Delta_g), \tag{3}$$

[22] Allred, Rosen, Tallmadge, and Williams, Rev. Sci. Instr. **22**, 191 (1951).
[23] C. L. Critchfield and D. C. Dodder, Phys. Rev. **75**, 419 (1949).

with

$$\Delta_g=\frac{b^2}{4L^2}\left[2\cot^2\theta-4+\frac{G+S}{R}\frac{2\cot\theta}{\sin\theta}+\frac{G^2+S^2}{R^2}(\cot^2\theta-\tfrac{1}{2})\right]$$

$$-\frac{h^2}{8R^2}+\frac{w^2}{3H^2}\left[-3-\left(\frac{D+J}{R}-\frac{D^2+J^2}{R^2}\right)\cot^2\alpha\right.$$

$$\left.\pm\left(\frac{D+J}{R}-2\frac{D^2+J^2}{R^2}\right)\cot|\alpha|\cot\theta+\frac{D^2+J^2}{R^2}\cot^2\theta\right]$$

$$+\frac{1}{\sigma}\frac{\partial\sigma}{\partial\theta}\left[\frac{b^2}{8L^2}\left(\frac{G^2+S^2}{R^2}-2\right)\cot\theta+\frac{h^2}{24R^2}\cot\theta\right.$$

$$\left.+\frac{w^2}{3HR}\left(1+\frac{2D}{H}\right)(\pm\cot|\alpha|-\cot\theta)\right]$$

$$+\frac{1}{\sigma}\frac{\partial^2\sigma}{\partial\theta^2}\left[\frac{b^2}{4L^2}+\frac{w^2}{3H^2}\right]. \quad (4)$$

It is assumed here that the swath scanned extends from a distance $h/2$ below to a distance $h/2$ above the intersection of the plate with the nominal scattering plane. The plate is slanted at an angle $|\alpha|$ ($\approx 5°$) with respect to the nominal direction of the scattered particles. The upper sign of the terms in $\cot|\alpha|$ are to be used for the slant shown in Fig. 1, where the inner half of the plate receives, on the average, particles scattered through a larger angle than the outer half. If the plates are slanted the opposite way, the lower sign is valid. All other symbols in Eq. (4) are defined in Fig. 1, with $G=S-L$ and $J=H+D$. For a very narrow collimator ($b=0$) and isotropic scattering ($\partial\sigma/\partial\theta=\partial^2\sigma/\partial\theta^2=0$), our expression agrees with the one given by Allred *et al.* For $\alpha=90°$, $D=0$, the geometry reduces to that considered by Critchfield and Dodder, except for the difference in the detector aperture. Here, it would be a rectangle of height h, width $2w$, whereas they treat a circle of radius a. The comparison is complicated by the fact that our term in w^2 includes the effects of both slits. The expressions agree as expected, however, if one puts $a^2=\frac{4}{3}w^2$ and $h=2w$.

The distance R is to be measured from the center of the scattering chamber to the intersection of the plate with the nominal scattering direction. This nominal center of the plate may not coincide with the geometric center if the plate is slightly misaligned. The deviation can be found by determining the ratio, r, of the intensities on the inner and outer (geometric) half of the plate and comparing it to the ratio, r^*, expected if the nominal center were at the geometric center. This ratio, obtained as a by-product in the calculation of the geometry correction, is

$$r^*=1+\frac{wH}{JR}(\cot|\alpha|\mp\cot\theta)\left(1+2\frac{D}{H}+\frac{4}{3}\frac{D^2}{H^2}\right)$$

$$\pm\frac{wH}{J^2}\frac{1}{\sigma}\frac{\partial\sigma}{\partial\theta}\left(1+\frac{8}{3}\frac{D}{H}+\frac{4}{3}\frac{D^2}{H^2}\right). \quad (5)$$

Here again the upper signs hold for the geometry of Fig. 1, the lower signs for plates of opposite slant. The distance R to be used in Eq. (3), then, is smaller than the distance to the geometric center of the plate by an amount

$$\Delta R\approx l_{\mathrm{eff}}(r-r^*)\cos\alpha/4, \quad (6)$$

where the effective length of the exposed swath is given by

$$l_{\mathrm{eff}}=wJ/H\sin\alpha. \quad (7)$$

APPENDIX B. CORRECTION FOR MULTIPLE SCATTERING

A correction formula for the effect of multiple scattering with foil targets has been given by Chase and Cox,[24] but it appears that no similar treatment for a gas target has been published. In the following calculation good geometry is assumed, i.e., the widths of the collimator and detector slits are neglected. Figure 17 shows the geometry used. The origin of the coordinate system is at the nominal scattering center. The incident particle travels in the $+y$ direction and is scattered in

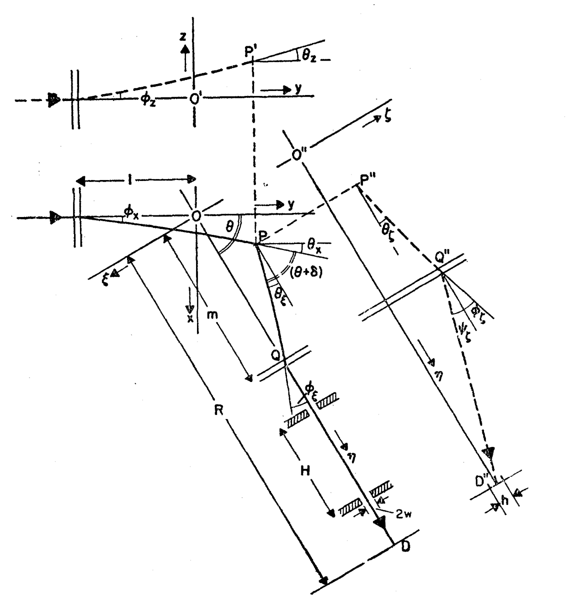

FIG. 17. Notation used in the calculation of the multiple-scattering correction. O=nominal scattering center and center of x, y, z and ξ, η, ζ coordinate systems. P=point in scattering volume element. Q=point where the scattered particle passes through the exit foil. D=detector. The plane view (x,y and ξ,η plane) and two projections (y,z and η,ζ planes) are shown.

[24] C. T. Chase and R. T. Cox, Phys. Rev. 58, 246 (1940).

the wall of the target chamber, at $y=-l$, through angles φ_x, φ_z. It arrives at the scattering volume $dx\,dy\,dz$ with projected deflections θ_x, θ_z. The scattered particle leaves the scattering volume in a direction deviating from the nominal one by θ_ξ, θ_ζ, is scattered in the gas so as to arrive at the exit window of the scattering chamber at coordinates $\xi_1\approx 0$, $\eta_1=m$ (chosen $\neq l$ for the sake of generality), and ζ_1, with angles φ_ξ and φ_ζ. Multiple scattering in the foil finally deflects the particle into the detector $[\psi_\xi\approx 0,\ \psi_\zeta=\zeta_1/(R-m)]$, i.e., through the second slit onto a swath of height h on the plate. After integrating over the (infinitesimal) slit widths and the swath height, one obtains the following expression for the intensity registered in the swath:

$$\begin{aligned}Y(\theta)=\frac{Nn4w^2h}{H(R-m)}\int & p(\varphi_x)p_{l+y}[x-(l+y)\varphi_x,\theta_x-\varphi_x]p(\varphi_z)\\ &\times P_{l+y}[z-(l+y)\varphi_z,\theta_z-\varphi_z]d\varphi_x d\varphi_z d\theta_x d\theta_z dxdydz\\ &\times\sigma(\theta+\delta)d\theta_\xi d\theta_\zeta P_{m-\eta}[-\xi-(m-\eta)\theta_\xi,\ \varphi_\xi-\theta_\xi]\\ &\times P_{m-\eta}[\zeta_1-z-(m-\eta)\theta_\zeta,\ \varphi_\zeta-\theta_\zeta]p(\psi_\zeta+\varphi_\zeta)\\ &\times p(-\varphi_\xi)\cos^2\psi_\zeta d\varphi_\xi d\varphi_\zeta d\zeta_1.\end{aligned}\quad(8)$$

The probability functions for multiple scattering in the foils, p, and in the gas, P, are taken from Rossi,[25] with slight changes in notation. The variation of the mean square scattering angle per unit path length, due to the energy loss in the gas, is neglected. The integration is tedious, but straightforward. The cross section $\sigma(\theta+\delta)$ is expanded in the vicinity of θ; wherever necessary, terms are expanded to second power of the deviation from the nominal scattering event. With Θ_w and Φ_w the rms angles in the entrance and exit window, Θ_g, Φ_g the rms angles in the gas over the distances l and m, and Θ_t the total rms angle, one obtains the final expression

$$I=\frac{Nn4w^2h}{HR\sin\theta}(1+\Delta_m),$$

with

$$\begin{aligned}\Delta_m=\cot^2\theta\Big[&\tfrac{1}{2}\Theta_t^2-\frac{m}{R}(\tfrac{1}{2}\Phi_g^2+\Phi_w^2)+\frac{l^2}{2R^2}(\tfrac{1}{3}\Theta_g^2+\Theta_w^2)\Big]\\ &+\frac{\cot\theta}{\sin\theta}\frac{l}{R}(\tfrac{1}{2}\Theta_g^2+\Theta_w^2)+(\cot^2\theta-1)\frac{m^2}{2R^2}(\tfrac{1}{3}\Phi_g^2+\Phi_w^2)\\ &-\frac{1}{\sigma}\frac{\partial\sigma}{\partial\theta}\frac{\cot\theta}{4}\Big[\Theta_t^2-\frac{l^2}{R}(\tfrac{1}{3}\Theta_g^2+\Theta_w^2)\\ &\qquad-\frac{m^2}{R^2}(\tfrac{1}{3}\Phi_g^2+\Phi_w^2)\Big]+\frac{1}{\sigma}\frac{\partial^2\sigma}{\partial\theta^2}\frac{\Theta_t^2}{4}.\end{aligned}\quad(9)$$

One may remark that no cross terms between the multiple-scattering and the geometry corrections are to be expected, if only terms up to the second power in the rms scattering angles (e.g., Θ_t) or geometric angles (e.g., w/H) are retained. Cross terms would have to be of the form $\Theta_t\times w/H$. Since the multiple-scattering correction for any good geometry chosen contains only quadratic terms in Θ_t, the subsequent integration for the finite geometry will not yield cross terms.

[25] B. Rossi, *High-Energy Particles* (Prentice-Hall, Inc., New York, 1952), p. 71.

PHYSICAL REVIEW VOLUME 116, NUMBER 5 DECEMBER 1, 1959

Reactions of Cu^{63} and Cu^{65} with Alpha Particles*

NORBERT T. PORILE AND DAVID L. MORRISON†
Chemistry Department, Brookhaven National Laboratory, Upton, New York
(Received July 10, 1959)

Excitation functions have been measured for the (α,n), $(\alpha,2n)$, and $(\alpha,\alpha n)$ reactions on Cu^{63} and Cu^{65}, as well as for the $Cu^{63}(\alpha,pn)$, $Cu^{65}(\alpha,2p)$, and $Cu^{65}(\alpha,2\alpha)$ reactions, for incident alpha particles of 15–41 Mev. The excitation functions for the (α,n), $(\alpha,2n)$, and (α,pn) reactions go through much sharper maxima than the excitation functions for the $(\alpha,\alpha n)$ reactions. Cross sections for the $(\alpha,2p)$ and $(\alpha,2\alpha)$ reactions increase monotomically with bombarding energy and attain values of 2.7 and 2.1 mb at 40 Mev, respectively. The value of $\sigma(\alpha,pn)/\sigma(\alpha,2n)$ for Cu^{63} in the region of maximum yield is 3.3. The maximum cross sections measured for the $(\alpha,\alpha n)$ reactions are 205 mb and 143 mb for Cu^{63} and Cu^{65}, respectively. The effects on the observed cross sections of neutron and proton binding energy differences, and of level density differences in the residual nuclei have been considered. The effect of these factors is in accord with the predictions of the statistical theory for the (α,n) and $(\alpha,2n)$ reactions but not for the $(\alpha,\alpha n)$ reaction.

A method for monitoring the energy of the incident beam based on the variation with energy of the ratio of cross sections for several of the above reactions is described.

I. INTRODUCTION

THE statistical theory of nuclear reactions indicates that the shape of the excitation functions as well as the magnitude of the cross sections for reactions induced by particles with incident energies less than 50 or 60 Mev should be determined by a large number of factors. These include the excitation energy of the compound nucleus, the binding energies of all particles that may be emitted at a given excitation energy, the

* Research performed under the auspices of the U. S. Atomic Energy Commission.
† Present address: Carnegie Institute of Technology, Pittsburgh, Pennsylvania.